ACS NANO

www.acsnano.org

ARTICLE

Engineered Cyanobacteria-Based Living Materials for Bioremediation of Heavy Metals Both In Vitro and In Vivo

Tao Sun,[▽] Huaishu Huo,[▽] Yingying Zhang,[▽] Yaru Xie, Yize Li, Kungang Pan, Fenfang Zhang, Jing Liu, Yindong Tong, Weiwen Zhang,* and Lei Chen*

Cite This: *ACS Nano* 2024, 18, 17694−17706

Read Online

ACCESS | Metrics & More | Article Recommendations | Supporting Information

ABSTRACT: The pollution caused by heavy metals (HMs) represents a global concern due to their serious environmental threat. Photosynthetic cyanobacteria have a natural niche and the ability to remediate HMs such as cadmium. However, their practical application is hindered by a low tolerance to HMs and issues related to recycling. In response to these challenges, this study focuses on the development and evaluation of engineered cyanobacteria-based living materials for HMs bioremediation. Genes encoding phytochelatins (PCSs) and metallothioneins (MTs) were introduced into the model cyanobacterium *Synechocystis* sp. PCC 6803, creating PM/6803. The strain exhibited improved tolerance to multiple HMs and effectively removed a combination of Cd^{2+}, Zn^{2+}, and Cu^{2+}. Using Cd^{2+} as a representative, PM/6803 achieved a bioremediation rate of approximately 21 μg of Cd^{2+}/OD_{750} under the given test conditions. To facilitate its controllable application, PM/6803 was encapsulated using sodium alginate-based hydrogels (PM/6803@SA) to create "living materials" with different shapes. This system was feasible, biocompatible, and effective for removing Cd^{2+} under simulated conditions of zebrafish and mice models. Briefly, in vitro application of PM/6803@SA efficiently rescued zebrafish from polluted water containing Cd^{2+}, while in vivo use of PM/6803@SA significantly decreased the Cd^{2+} content in mice bodies and restored their active behavior. The study offers feasible strategies for HMs bioremediation using the interesting biomaterials of engineered cyanobacteria both in vitro and in vivo.

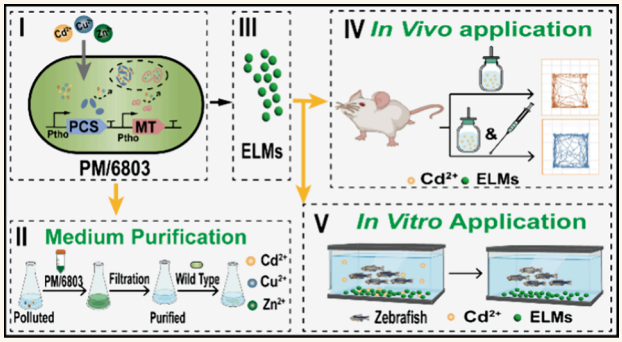

KEYWORDS: *cyanobacteria, heavy metals, bioremediation, metal chelators, engineered living materials*

Heavy metals (HMs) are typically metallic chemical elements with a high density and toxicity at low concentrations. Although HMs occur naturally on Earth, rapid industrialization and urbanization have led to severe environmental pollution.[1] Specifically, chemicals containing cadmium (Cd), copper (Cu), lead (Pb), zinc (Zn), mercury (Hg), and chromium (Cr) are released into the soil and hydrosphere, causing increasing ecological and global public health concerns.[2] HMs like Cd have no physiological function but act as toxicants and carcinogens that affect the kidneys and skeleton.[3] Generally, Cd released into the environment can originate from copper and nickel smelting and refining, fossil fuel combustion, and the use of phosphate fertilizers.[4] In addition, Cd is widely employed as a stabilizer in plastics, color pigments, and Ni−Cd batteries, whose wastes worsen environmental pollution.[3] It is worth noting that Cd has been a concern for the European Union since the 1970s, and safe exposure levels for food have been established by World Health Organization and the Food and Agriculture Organization (United Nations Environment Programme: https://www.unep.org/topics/chemicals-and-pollution-action/pollution-and-health/heavy-metals/cadmium). Generally, Cd occurs in soil as Cd^{2+} at concentrations typically ranging from 0.1 to 1.0 mg/kg.[5] Weathering can lead to Cd concentrations up to 5 μg/L in soil water and up to 1 μg/L in groundwater.[4] The concentrations, however, can exceed the permissible limits in various environments due to pollution, thereby surpassing the threshold set for health safety. For example, the

Received: February 22, 2024
Revised: June 15, 2024
Accepted: June 17, 2024
Published: June 27, 2024

https://doi.org/10.1021/acsnano.4c02493
ACS Nano 2024, 18, 17694−17706

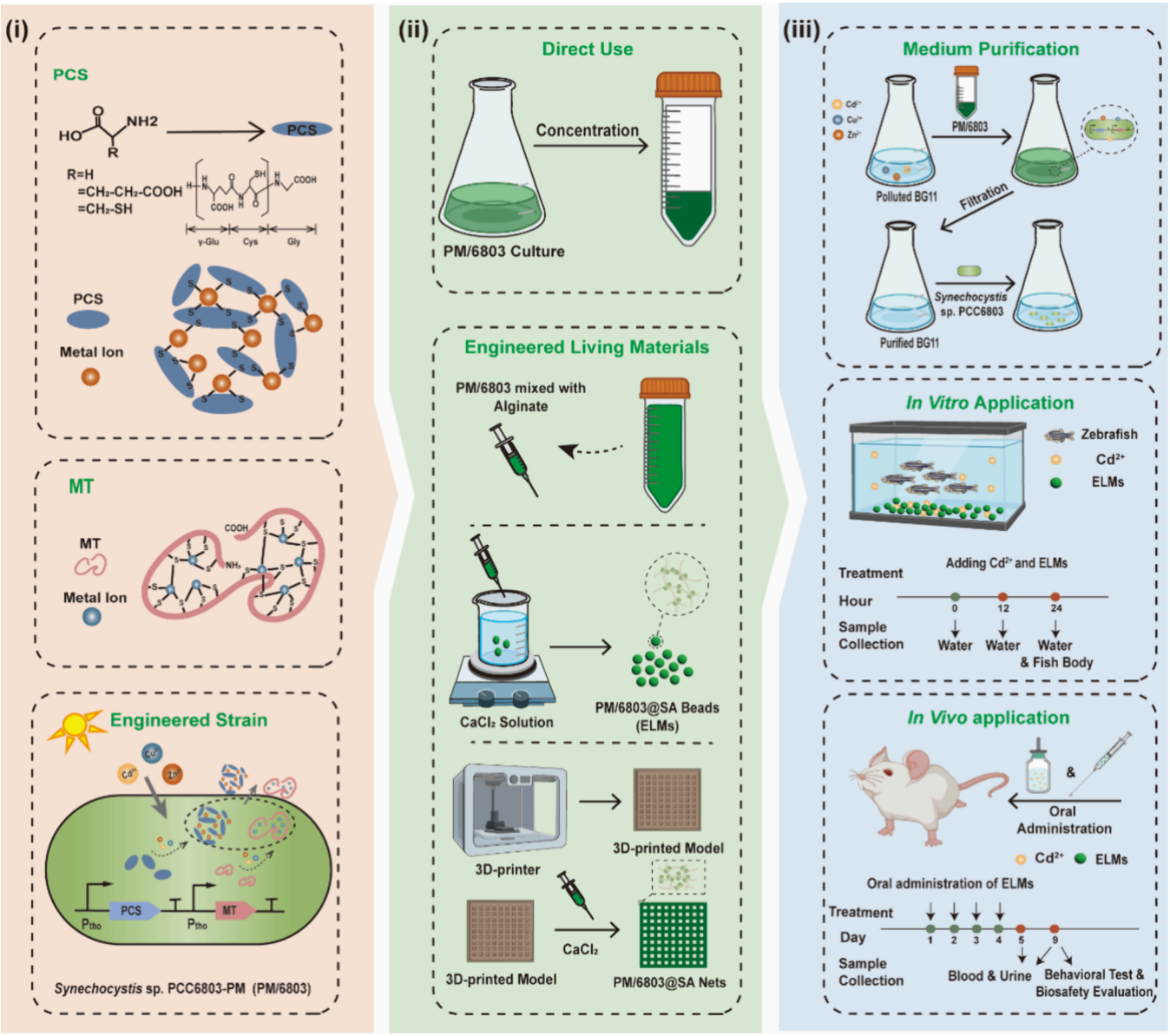

Figure 1. Schematic of this study. Briefly, (i) chelator proteins for HMs were introduced into *Synechocystis* sp. PCC 6803; (ii) the engineered strain could be used directly via centrifugation collection or packaged into engineered living materials; (iii) three samples include medium purification, zebrafish, and mice models.

concentrations of Cd^{2+} in wastewater and soil reached levels as high as 2 mg/L (about 17.8 μM) and 140 mg/kg, respectively, in specific areas of Pakistan.[6] In addition, the rice paddies (1−10 mg of Cd/(kg of soil)) were irrigated with Cd-contaminated water sourced from the Jinzu River, which had been affected by metal mining activities in Japan during the early 1950s. This irrigation practice resulted in the occurrence of a severe bone disease known as *itai*−*itai* disease.[5] Consequently, developing an efficient and low-cost strategy to treat HMs pollution such as Cd is of vital importance.

Traditionally, chemical and physical methods for heavy metal removal are often costly and less efficient, generating large quantities of toxic sludge.[7] In contrast, bioremediation using microorganisms such as bacteria, microalgae, and yeast is a promising, eco-friendly, and cost-effective alternative.[8−10] Among them, autotrophic cyanobacteria are the only prokaryotes capable of oxygenic photosynthesis, thereby occupying an important ecological niche and accounting for approximately 25% of the annual carbon fixation on earth.[11] In addition, cyanobacteria have great potential for bioremediation due to their naturally high binding affinity and rich binding sites for HMs. For example, alginate immobilized *Nostoc calcicola* HH-12 and *Chroococcus* sp. HH-11 showed more than 50% removal of 20 mg/L Cr^{6+} within 30 min.[12] In addition, Rezasoltani and Champagne realized 85.0% removal of Pb^{2+} up to 60 mg/L using *Anabaena* sp. after 12 days.[13] However, bioremediation capabilities of cyanobacteria are restricted by their limited tolerance to most of the HMs.[14,15] For instance, the adsorption efficiency of *Synechocystis* sp. PCC 7806 reached ∼75.4% against a 10 mg/L Cr^{3+} solution; it was drastically decreased at 20 mg/L Cr^{3+} due to significantly arrested growth.[16] The cyanobacterium *Synechocystis* sp. PCC 6803 has been fully sequenced and is widely employed as a model organism due to its ease of gene manipulation.[15,16] Generally, the growth of *Synechocystis* sp. PCC 6803 can be inhibited by approximately 50% when exposed to 4.6 μM

https://doi.org/10.1021/acsnano.4c02493
ACS Nano 2024, 18, 17694−17706

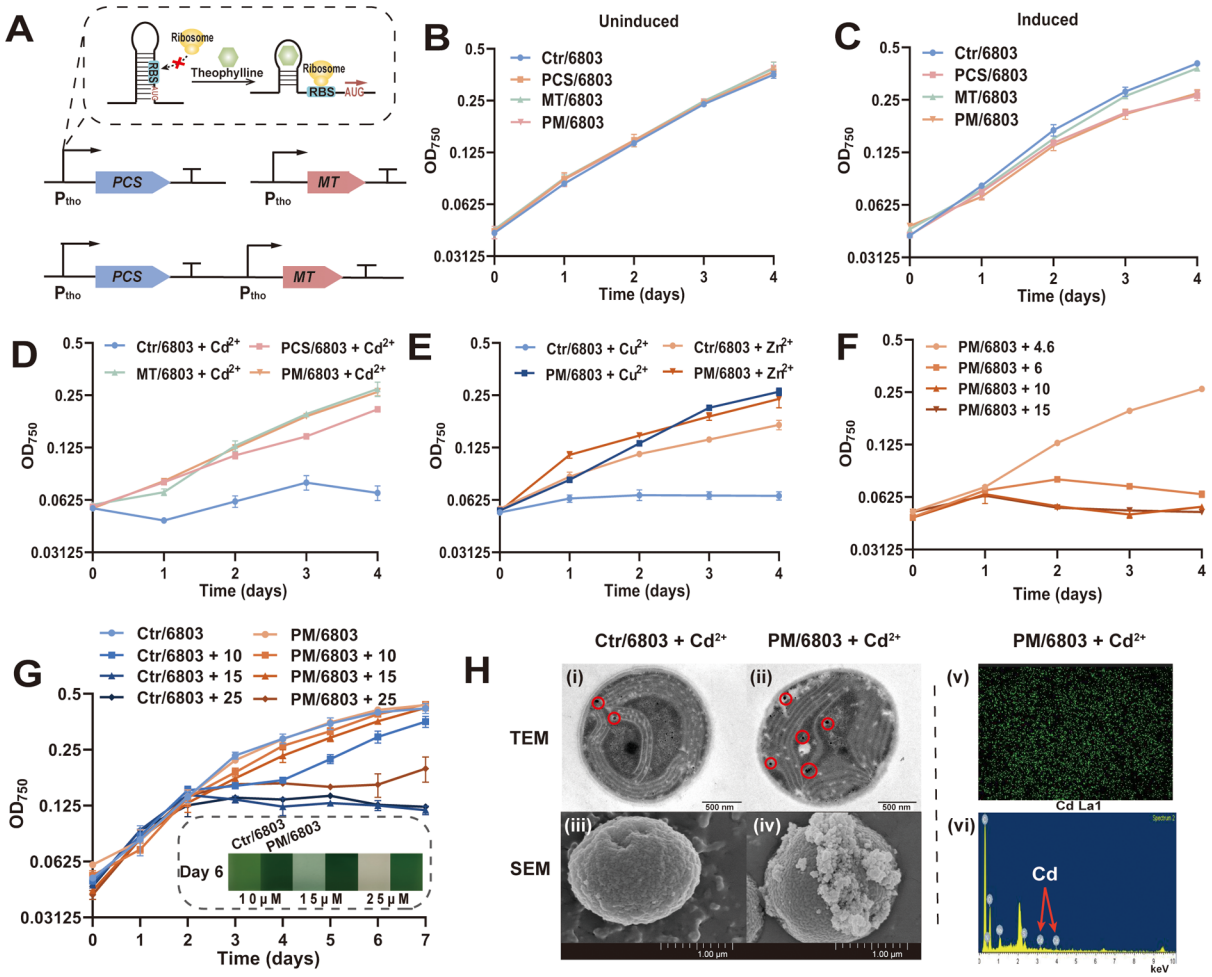

Figure 2. Enhanced tolerance to HMs via overexpressing genes encoding PCS and MT. (A) Schematic of the strain construction. The expression of the exogenous gene was controlled via a theophylline-responsive riboswitch. In detail, the RBS region would be isolated due to the secondary structure of the riboswitch without induction and be exposed after induction with theophylline due to the conformational change. (B) Growth patterns of Ctr/6803, MT/6803, PCS/6803, and PM/6803 under normal BG11 medium without theophylline induction. OD_{750} represented the optical density of the strains at 750 nm, which is an indicator of their cell density. (C) Growth patterns of Ctr/6803, MT/6803, PCS/6803, and PM/6803 under normal BG11 medium with 2 mM theophylline induction at day 0. (D) Growth patterns of Ctr/6803, MT/6803, PCS/6803, and PM/6803 under BG11 medium (pH = 9) with 2 mM theophylline induction and 4.6 μM Cd^{2+} at 0 h. (E) Growth patterns of Ctr/6803 and PM/6803 under BG11 medium with 2 mM theophylline induction and 6 μM Cu^{2+} or 3 μM Zn^{2+} at day 0. (F) Growth patterns of PM/6803 under BG11 medium with 2 mM theophylline induction and 4.6, 6, 10, and 15 μM Cd^{2+} at day 0 (shown as PM/6803 + 4.6, PM/6803 + 6, PM/6803 + 10, and PM/6803 + 15). (G) Growth patterns of Ctr/6803 and PM/6803 under BG11 medium with 2 mM theophylline induction and 10, 15, and 25 μM Cd^{2+} at day 2 (shown as Ctr/6803 + 10, Ctr/6803 + 15, Ctr/6803 + 25, PM/6803 + 10, PM/6803 + 15, and PM/6803 + 25). The pictures showed the visual bacterial color of different strains on day 6. (H) ((i), (ii)), TEM analysis of Ctr/6803 and PM/6803 with 10 μM Cd^{2+} treatment; ((iii), (iv)), SEM analysis of Ctr/6803 and PM/6803 with 10 μM Cd^{2+} treatment; ((v), (vi)) energy dispersive spectroscopy analysis of the extracellular substances from PM/6803 with 10 μM Cd^{2+} treatment.

Cd^{2+}.[17] Toth et al. demonstrated that the toxic effects of Cd^{2+} on *Synechocystis* sp. PCC 6803 involved the rapid inhibition of CO_2-dependent electron transport, followed by inhibitory influences on PS II electron transport and the degradation of the reaction center protein D1.[18] These results underscore the need to develop a preferable cyanobacterial chassis with enhanced tolerance and chelating abilities toward HMs.

Phytochelatins (PCSs) and metallothioneins (MTs) are the most important types of metal chelators, capable of withstanding high concentrations of HMs and chelating them.[19] Previously, Choi et al. demonstrated the efficiency of these two chelator proteins by coexpressing PCS and MT in *Escherichia coli* to synthesize various metal nanomaterials.[20] Meanwhile, cyanobacteria-based living materials have garnered attention due to their captivating applications in structural materials, wound healing, tumor treatment, and hypoxia alleviation.[21−24] Taken together, the development of living materials involving engineered cyanobacteria with additional expressed metal chelators could simultaneously enhance the tolerance of cyanobacteria to heavy metals (HMs) and facilitate their controlled release during application. Building upon these hypotheses, PCS and MT respectively from *Arabidopsis thaliana*[25] and *Pseudomonas*[26] were selected in this study due to their chelating ability specifically for heavy metals like Cd^{2+}, Zn^{2+}, etc. We integrated genes encoding PCS and MT into the model cyanobacterium *Synechocystis* sp. PCC 6803 and explored their roles in tolerance and bioremediation of HMs, particularly Cd^{2+}, through several compelling examples in this

https://doi.org/10.1021/acsnano.4c02493
ACS Nano 2024, 18, 17694−17706

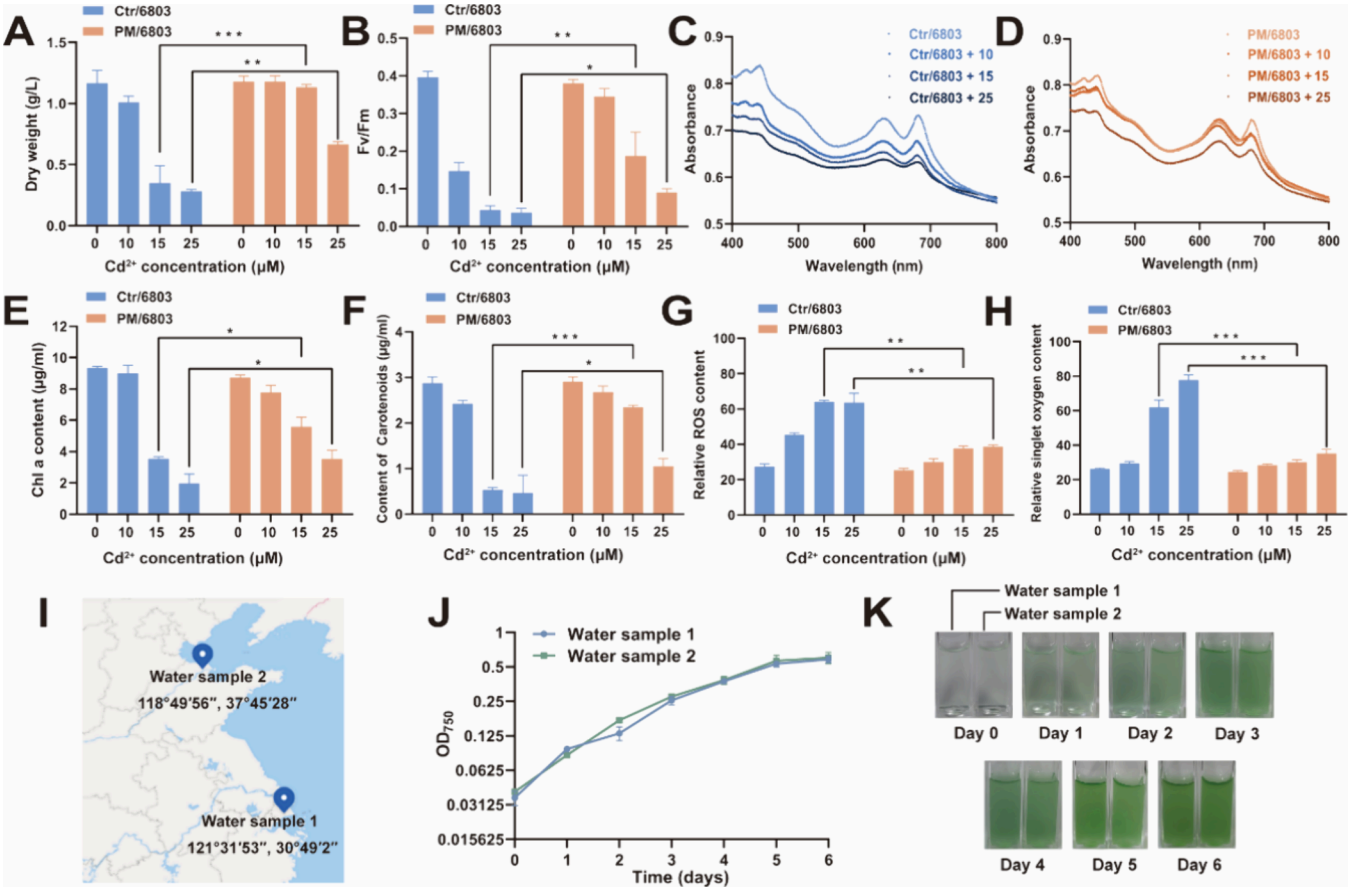

Figure 3. Physiological responses of PM/6803 to Cd^{2+} and its growth in natural water. Dry weight (A), F_v/F_m (B), absorption spectra (C, D), Chl *a* (E), carotenoids (F), ROS (G), and singlet oxygen (H) measurement in Ctr/6803 and PM/6803 under 0, 10, 15, and 25 μM Cd^{2+} added at day 2. (I) Location site of the natural water sample. Growth patterns (J) and pictures (K) of PM/6803 under two natural water samples. (*p < 0.05, **p < 0.01, and ***p < 0.001 by Student's t test).

study (Figure 1). Notably, a significant resistance to Cd^{2+}, Cu^{2+}, and Zn^{2+} was achieved in the engineered strain along with the improved bioremediation ability. Furthermore, the engineered strain was encapsulated using alginate-based hydrogels to create "living materials", promoting its stable and controllable application. Using Cd^{2+} as a proof of concept, the roles of engineered living materials in Cd^{2+} removal were evaluated using zebrafish and mice models.

RESULTS

Enhanced Tolerance to Cd^{2+}, Cu^{2+}, and Zn^{2+} via Overexpressing Genes Encoding PCS and MT. To investigate the potential roles of PCS and MT on cyanobacterial tolerance against HMs, genes encoding PCS and MT used previously[20] were individually or combinedly expressed under the control of a theophylline-responsive riboswitch (the working principle was described in the figure legends) using a shuttle vector pJA2 in wild type strain of *Synechocystis* sp. PCC 6803 (wild type strain was the original strain without any modifications), leading to the strains including PCS/6803, MT/6803, and PM/6803 (containing both PCS and MT) (Figure 2A; Supporting Information Tables S1 and S2). Successful transformation and expression of PCS and MT were validated via PCR and SDS-PAGE, respectively (Figure S1A,B). Meanwhile, an empty pJA2 plasmid was introduced into the wild type to make a control strain named Ctr/6803. All four strains exhibited similar growth patterns without induction (Figure 2B). Slight growth defects in PCS/6803 and PM/6803 were observed compared to those in Ctr/6803 and MT/6803 with 2 mM theophylline induction, indicating the potential metabolic burden of PCS in *Synechocystis* sp. PCC 6803 (Figure 2C).

For a proof of concept, Cd^{2+} stress was selected due to its high carcinogenicity to humans and severe toxicity to cyanobacteria.[15,27] As a result, though the four strains exhibited no significant differences toward 4.6 μM Cd^{2+} under normal BG11 medium (pH = 7.5; data not shown), enhanced tolerance of PCS/6803, MT/6803, and PM/6803 was observed compared to that of Ctr/6803 under BG11 with pH = 9 (Figure 2D). The results were consistent with the previous study in *E. coli*, which found the bioremediation of metal ions was pH-dependent.[20] Meanwhile, changed pH did not alter the normal growth of all constructed strains (Figure S2A). Notably, both PCS and MT seemed to contribute to the Cd^{2+} tolerance, as their combination showed a synergistic effect. Thus, PM/6803 was utilized to test its tolerance to other HMs. Among the tested HMs, increased tolerance of PM/6803 to 6 μM Cu^{2+} or 3 μM Zn^{2+} compared to that of Ctr/6803 was observed (Figure 2E). These results demonstrated that the expression of PCS and MT improved the tolerance of *Synechocystis* sp. PCC 6803 to multiple HMs.

To explore the resistance limit, PM/6803 was cultivated under Cd^{2+} stress at increasing concentrations. Unfortunately, we found that 6 μM Cd^{2+} was lethal to PM/6803 with an

https://doi.org/10.1021/acsnano.4c02493
ACS Nano 2024, 18, 17694−17706

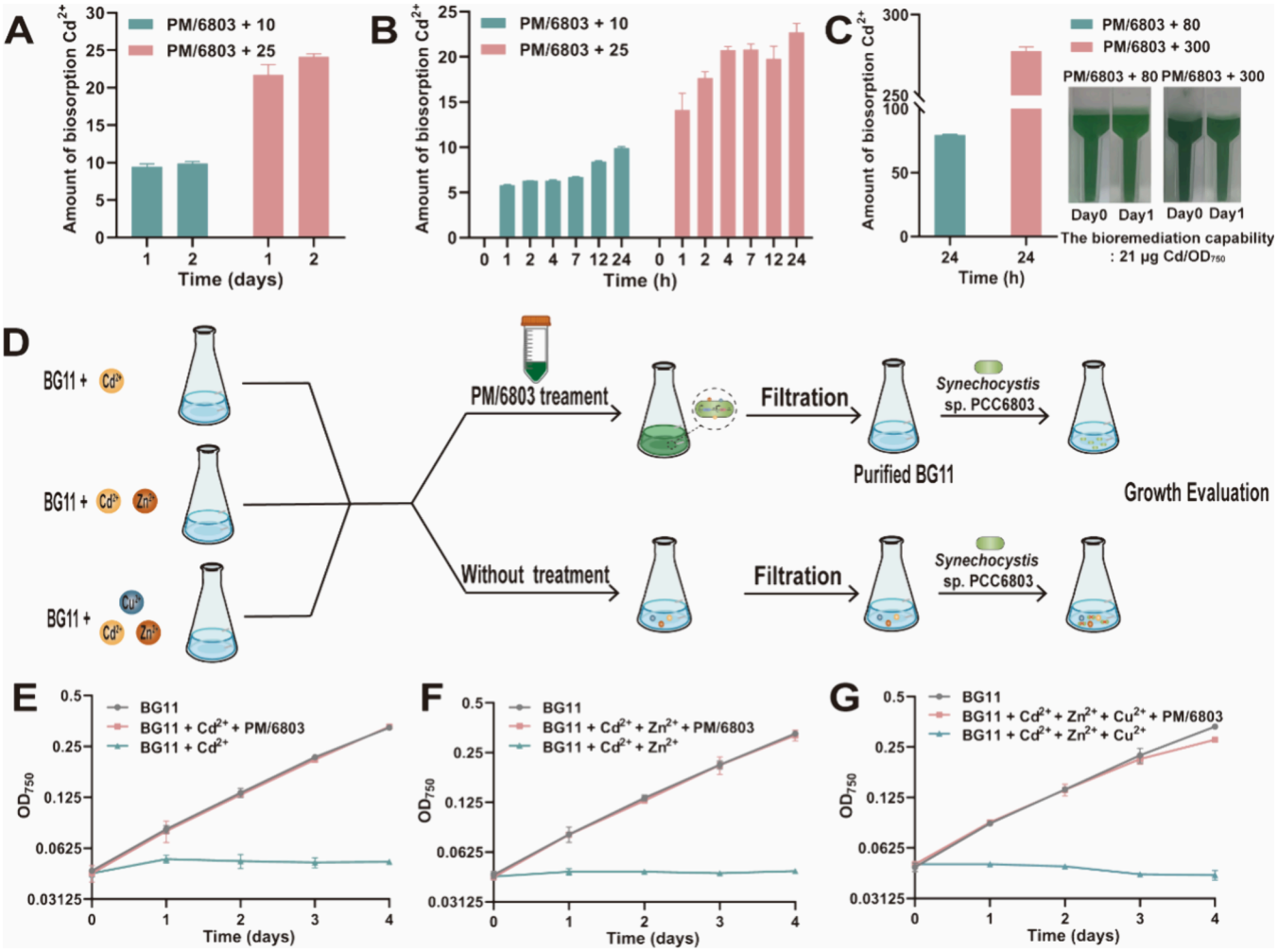

Figure 4. Evaluation of bioremediation capability of PM/6803. (A) Measurement of adsorbed Cd^{2+} in PM/6803 under 10 and 25 μM Cd^{2+} conditions in the first and second days (shown as PM/6803 + 10 and PM/6803 + 25). (B) Measurement of adsorbed Cd^{2+} in PM/6803 under 10 and 25 μM Cd^{2+} conditions in the first day (shown as PM/6803 + 10 and PM/6803 + 25). (C) Measurement of adsorbed Cd^{2+} and the phenotype picture in PM/6803 under 80 and 300 μM Cd^{2+} conditions in the first day (shown as PM/6803 + 80 and PM/6803 + 300). (D) Schematic used PM/6803 for medium purification. (E) Growth patterns of wild type *Synechocystis* sp. PCC 6803 in normal medium, medium with 15 μM Cd^{2+} with (shown as BG11+ Cd^{2+} + PM/6803) or without (shown as BG11 + Cd^{2+}) purification. (F) Growth patterns of wild type *Synechocystis* sp. PCC 6803 in normal medium, medium with 15 μM Cd^{2+} and 6 μM Cu^{2+} with (shown as BG11 + Cd^{2+} + Cu^{2+} + PM/6803) or without (shown as BG11 + Cd^{2+} + Cu^{2+}) purification. (G) Growth patterns of wild type *Synechocystis* sp. PCC 6803 in normal medium, medium with 15 μM Cd^{2+}, 6 μM Cu^{2+}, and 3 μM Zn^{2+} with (shown as BG11 + Cd^{2+} + Cu^{2+} + Zn^{2+} + PM/6803) or without (shown as BG11 + Cd^{2+} + Cu^{2+} + Zn^{2+}) purification.

initial inoculation OD_{750} of 0.04 (Figure 2F). It was probably due to the toxicity of Cd^{2+}, the lower initial inoculum, and the potential metabolic burden of PCS. To address the issue, the Cd^{2+} stock and theophylline inducer were added into the culture at the second day instead of day 0 (the same condition was also used in the next section). As expected, enhanced tolerance to Cd^{2+} up to 25 μM was realized in PM/6803, which was totally lethal to Ctr/6803 (Figure 2G). Furthermore, to evaluate whether Cd^{2+} was chelated, transmission electron microscope (TEM), scanning electron microscope (SEM), and elements analysis were performed for PM/6803 with or without Cd^{2+} treatment. Black dots resulted from inorganic substances could be observed in both Ctr/6803 and PM/6803 (red circles in Figure 2H(i,ii)), suggesting the natural roles of *Synechocystis* sp. PCC 6803 for Cd^{2+} bioremediation. Second, SEM analysis found the surface of Ctr/6803 was generally smooth, while significant aggregates existed in the cell surface of PM/6803 (Figure 2H(iii,iv)). Elements analysis identified accumulation of Cd in the extracellular substances of PM/6803 (Figure 2H(v,vi)) but not in the Ctr/6803 (Figure S2B), suggesting that chelated Cd existed both intracellularly and extracellularly in PM/6803. The results were consistent with the previous reports that HMs chelated by algae would be isolated into vacuoles or out of cells through membrane transporters.[28] In addition, the results suggested PM/6803 had a better ability for Cd^{2+} bioremediation than Ctr/6803.

Exhibition of the Engineered Strain to Cd^{2+} Stress and under Natural Water. The stable property of engineered strain under HM conditions is crucial for bioremediation. Cd^{2+} is known to affect the photosystems of both cyanobacteria and plants.[29] For *Synechocystis* sp. PCC 6803, quantum yields of photosystem II and photosystem I were found decreased under the Cd stress, which could not be fully protected by inherent photoprotection mechanisms.[30] Generally, we found that PM/6803 could accumulate similar

https://doi.org/10.1021/acsnano.4c02493
ACS Nano 2024, 18, 17694−17706

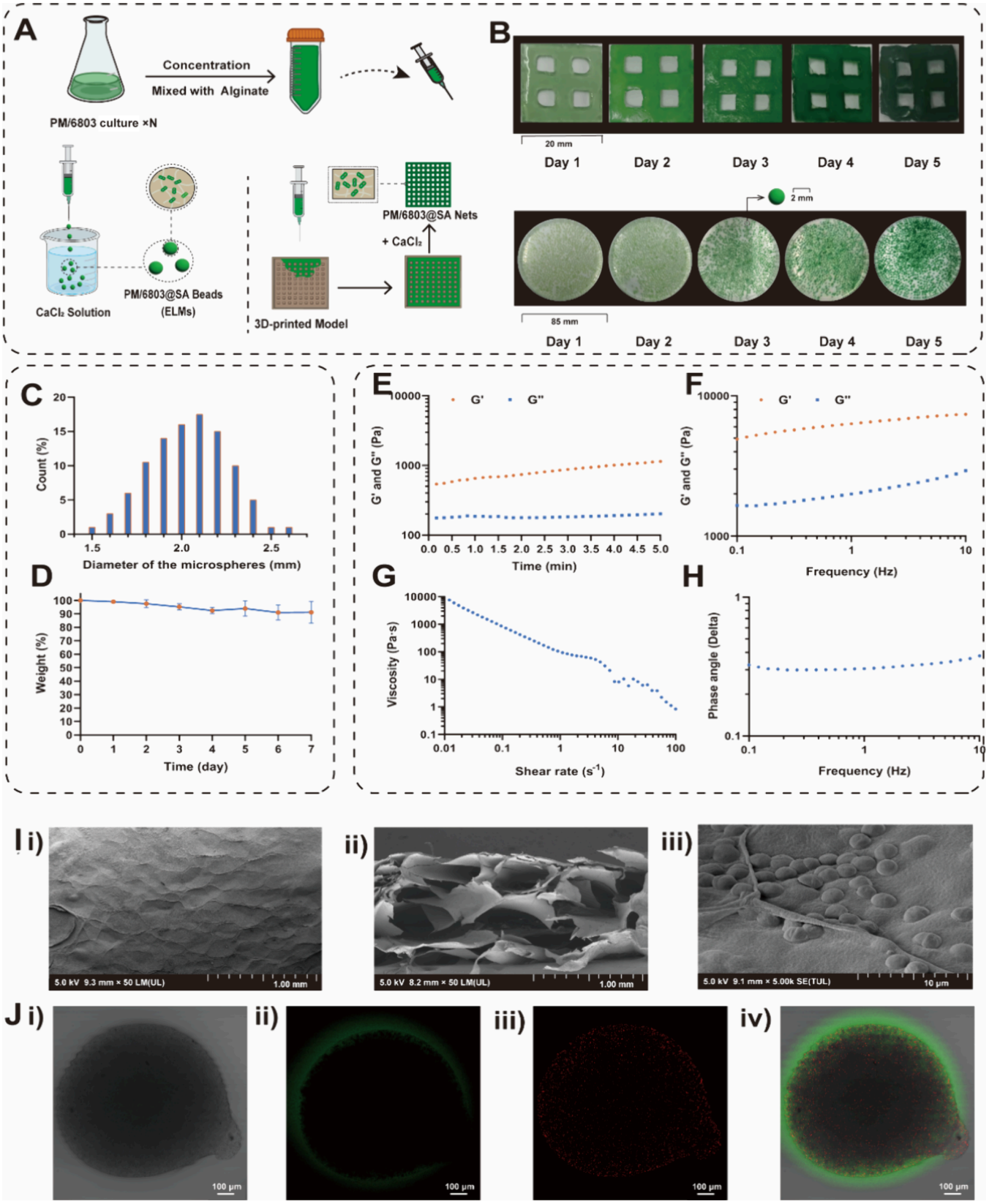

Figure 5. Characterization of PM/6803@SA. (A) Schematic of the creation of engineered living materials. (B) Growth of PM/6803 in packaged hydrogels growing in liquid BG11 medium. (C) Size distributions of the PM/6803@SA beads. (D) Weight change of PM/6803@SA beads.(E−H) Rheological analysis of PM/6803@SA beads. (I) Surface morphology and section characterization of PM/6803@SA beads via SEM. (J) Fluorescence images of the PM/6803@SA beads: (i) the image, (ii) fluorescence of the bead, (iii) autofluorescence of PM/6803, and (iv) overlay of panels ii and iii. The beads were stained with calcein (green), and PM/6803 was observed by chlorophyll autofluorescence (red).

https://doi.org/10.1021/acsnano.4c02493
ACS Nano 2024, 18, 17694−17706

biomass under 0, 10, and 15 μM Cd^{2+} conditions, while it decreased by about 44% under 25 μM Cd^{2+} condition (Figure 3A). Differently, biomass of Ctr/6803 began to decrease under 10 μM Cd^{2+} condition and decreased by about 76% under 15 μM Cd^{2+} condition (Figure 3A). To evaluate the stability of the engineered strain, physiological parameters of Ctr/6803 and PM/6803 were measured under 10, 15, and 25 μM Cd^{2+} conditions. As mentioned above, Cd^{2+} was harmful to cyanobacterial photosystem II, which could be evaluated from the ratio of F_v/F_m (representing the maximum quantum yield of photosystem II). As illustrated in Figure 3B, the F_v/F_m ratio in PM/6803 could still maintain about 51% under 15 μM Cd^{2+} (to that under 0 μM Cd^{2+}), while it sharply decreased to almost zero in Ctr/6803. Furthermore, absorption spectra of Ctr/6803 and PM/6803 were measured to explain the changes of F_v/F_m under Cd^{2+} stress. Absorption peaks of the main pigments like chlorophyll and carotenoids were significantly reduced in Ctr/6803 caused by 15 μM Cd^{2+}, while they remained almost the same as 0 μM Cd^{2+} in PM/6803 (Figure 3C,D). Consistently, quantitation of Chl *a* and carotenoids demonstrated their decrease in Ctr/6803 and maintenance in PM/6803 under 15 μM Cd^{2+} (Figure 3E,F). Finally, the contents of reactive oxygen species (ROS) and singlet oxygen were measured in Ctr/6803 and PM/6803 as their accumulation could be triggered by HMs and lead to cell death. As expected, both ROS and singlet oxygen could stay at a relative low level in PM/6803 even under 25 μM Cd^{2+}, while they gradually increased in Ctr/6803 with 10 μM Cd^{2+} (Figure 3G,H). All of these results suggested that PM/6803 was more resistant to Cd^{2+} than Ctr/6803.

To evaluate whether PM/6803 could be used in natural water, we also investigated its stability using water taken from two Chinese estuaries belonging to the Yellow River and Yangtze River (Figure 3I). As shown in Figure 3J,K, PM/6803 could maintain growth patterns similar to that grown in BG11 medium (Figure 2B), indicating it could survive under natural hydrosphere. Therefore, PM/6803 could possess application potential in natural environments after careful biosafety evaluation and/or critically controlled release in the future.

Evaluation of the Bioremediation Efficiency and Capability of PM/6803 to Cd^{2+}. We quantificationally deduced the efficiency and capability of PM/6803 in bioremediation via tracking the content of Cd^{2+} in the medium. We calculated the adsorbed Cd^{2+} after treatment with PM/6803, finding that 10 μM Cd^{2+} was chelated within 1 day and 25 μM Cd^{2+} was totally chelated within 2 days (Figure 4A). Then we recorded the temporal absorption of Cd^{2+} in the first day to evaluate the efficiency. As shown in Figure 4B, about 58 and 56% Cd^{2+} were chelated in the first hour under 10 and 25 μM Cd^{2+} conditions, respectively, and its content kept decreasing over time. To estimate the limit for Cd^{2+}, we evaluated whether the increased populations of PM/6803 could continue to enhance its bioremediation capability. To explore whether the absorption of Cd^{2+} was stable, we killed PM/6803 via high temperature after treatment. Then the dead strain was kept in the original simulative wastewater for 5 days. After that we found the content of Cd^{2+} remained almost stable in the wastewater (Figure S5), suggesting the chelating of PM/6803 for Cd^{2+} was tight and the bioremediation was stable. Interestingly, we found PM/6803 with a density of OD_{750} = 0.7 (20 mL) could resist and chelate 80 μM Cd^{2+} within 1 day (Figure 4C). Encouraged by this result, we further demonstrated that ~93% of 300 μM Cd^{2+} could still be chelated by PM/6803 with a density of OD_{750} = 1.5 (10 mL) (Figure 4D), suggesting an approximate bioremediation capability of about 21 μg of Cd^{2+}/OD per day.

We then evaluated the effects of bioremediation via comparing the growth of wild type *Synechocystis* sp. PCC 6803 in HM(s)-wasted medium with or without the treatment of treated PM/6803. In detail, medium containing 15 μM Cd^{2+} was treated with PM/6803 or Ctr/6803 (collected from 25 mL of culture with OD_{750} = 0.6) for 1 day and then the purified medium was obtained via filtration (Figure 4D). The growth of the wild type in untreated medium and purified medium was recorded. As expected, the untreated medium was lethal to wild type, but they could support the normal growth of wild type after treatment with PM/6803 (Figure 4E). On the contrary, the medium still could not support the growth of wild type after treatment with Ctr/6803 (Figure S4A), suggesting its ability for bioremediation was not enough. Then the recycle use of PM/6803 was investigated and we found that the reclaimed strain of PM/6803 could be reused at least three times using the above model (Figure S4B). Finally, the role of PM/6803 in treating a combination of 15 μM Cd^{2+} and 6 μM Cu^{2+} or 15 μM Cd^{2+}, 6 μM Cu^{2+}, and 3 μM Zn^{2+} (collected from 25 mL of culture with OD_{750} = 1.2) was also tested (Figure 4D). Similarly, PM/6803 was also demonstrated to be effective for treating multiple HMs (Figure 4F,G), preliminarily indicating it could be utilized for the bioremediation of HMs.

Characterization of the Engineering Living Materials PM/6803@SA. To explore the practical applications of PM/6803, its easy use and recyclability were important factors that needed to be considered. Hydrogels based on alginate have been demonstrated to be feasible for packaging cyanobacteria to make "living materials" in our previous studies.[21,31] The living materials could be created into different shapes to satisfy specific application scenarios via changing the models (Figure 5A). In this study, sodium alginate-based hydrogels were used to package PM/6803 (PM/6803@SA) to make beads or nets. We demonstrated that PM/6803 could survive well after being packaged in hydrogels, as their visible color and spontaneous chlorophyll fluorescence increased with the extension of culture time (Figure 5B and S6A). Meanwhile, effects of PM/6803@SA with different shapes for Cd^{2+} bioremediation were validated using simulative wastewater polluted by Cd^{2+}. Beads of PM/6803@SA were chosen in further study due to their superior effects (Figure S6B). To characterize the performance of PM/6803@SA beads, their size distribution and weight change with time were measured (Figure 5C,D). Then the rheology analysis indicated that the structure of beads was maintained stable (Figure 5E,F). In addition, they exhibited pseudoplastic behavior and good elastic properties (Figure 5G,H). Further, the characterization of the beads was measured using SEM, which indicated the porous structure of the hydrogel and the uniform distribution of PM/6803 (Figure 5I). In addition, we also investigated the hydrogels using a confocal microscope based on staining the beads with calcein and spontaneous chlorophyll fluorescence of PM/6803; founding PM/6803 was alive and evenly distributed in the beads (Figure 5J).

In Vitro Application of the Engineered Strain for Cd^{2+} Bioremediation Using Zebrafish Model. Then, we used zebrafish models grown in Cd^{2+}-contaminated water to evaluate the efficiency of PM-6803. Briefly, 5 groups of zebrafish (each group had a total of 15 zebrafish divided into 3

https://doi.org/10.1021/acsnano.4c02493
ACS Nano 2024, 18, 17694−17706

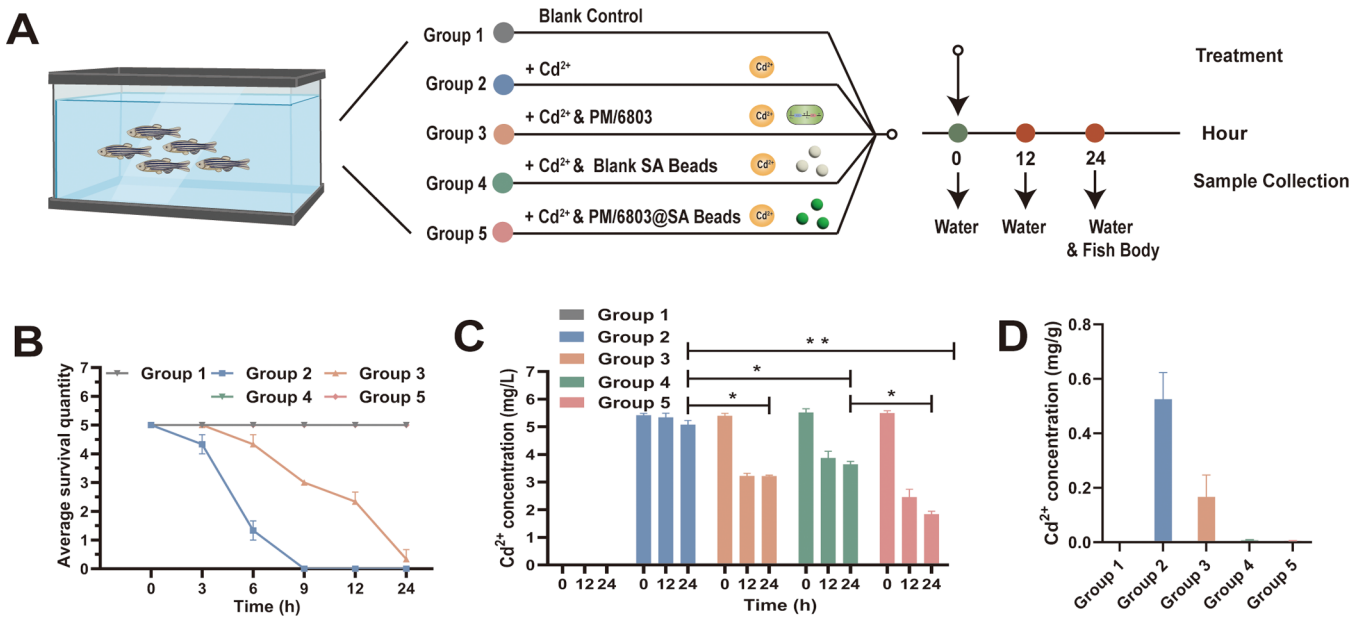

Figure 6. Application of PM/6803@SA for Cd^{2+} bioremediation using zebrafish model. (A) Schematic of the evaluation of PM/6803 in Cd^{2+} bioremediation using zebrafish model. (B) Average live quantity of zebrafish in different groups. (C) Concentrations of Cd^{2+} in the water of different groups at 0, 12, and 24 h. (D) Concentrations of Cd^{2+} in the main body of zebrafish in different groups at 24 h.

subgroups) were cultivated in water containing 5 mg/L Cd^{2+}, leading to an acute exposure. PM/6803 was added directly (Group 3) or packaged in hydrogels (Group 5), while untreated Group 2 and treated with blank hydrogels (Group 4) were used as the control (Figure 6A). Zebrafish grown in normal water without Cd^{2+} were taken as a positive control (Group 1). As a result, we found that 5 mg/L Cd^{2+} was extremely toxic to zebrafish as all of them died within 9 h in Group 2 (Figure 6B). Surprisingly, direct use of PM/6803 only alleviated the death rate (though 1 fish survived in Group 3), while all zebrafish survived in Groups 4 and 5 (Figure 6B). Via determining the concentrations of Cd^{2+} in the water, we found its concentration maintained stable in Group 2 but was decreased by about 40, 34, and 67% in Groups 3, 4, and 5 in 24 h, respectively (Figure 6C). It was not surprising that Cd^{2+} decreased in Group 4 as alginate was able to chelate metals.[32] Though the remaining Cd^{2+} in Group 3 is significantly lower than that in Group 4, survival of zebrafish in Group 3 was not improved. We speculated that zebrafish in Group 3 ate the PM/6803 (uniformly dispersed in the water) containing chelated Cd, thus leading to their indirect uptake of Cd. For PM/6803@SA, the beads sank into the bottom, thus excluding the predation by zebrafish. Finally, the Cd content in the main body (without head and tail) of zebrafish was measured at 24 h. As illustrated in Figure 6D, the acute exposure led to the fast accumulation of Cd^{2+} in zebrafish of Group 2 but significantly decreased in that of Group 3. Meanwhile, Cd in zebrafish of Groups 4 and 5 was not detectable, suggesting the protection from alginate beads alone or its combination with PM-6803. In conclusion, the package of PM-6803 in hydrogels made it both controllable and easily recycled and realized a synergetic effect with alginate for bioremediation.

In Vivo Application of the Engineered Strain for Cd^{2+} Bioremediation Using Mice Model. Encouraged by the in vitro results using zebrafish mentioned above, we evaluated whether packaged PM/6803 could be used for Cd^{2+} bioremediation in vivo using mice models as cyanobacteria have been demonstrated biocompatible and effective in treating multiple diseases including tumor,[21] ischemic heart,[22] wound healing,[33] or brain rescue[34] in mice or tadpoles. In this case, 25 mice were divided into 5 groups (Figure 7A), among which Group 1 was the normal control group, while Group 5 was fed with packaged PM/6803 only for biosafety evaluation. In addition, Group 2, Group 3, and Group 4 were fed with water containing 5 mg/L Cd^{2+} for continuous 4 days via oral administration. Meanwhile, Group 3 was fed packaged Ctr/6803, while Group 4 was fed packaged PM/6803 via oral administration. Though the body weights seemed similar during the tested period (Figure 7B), concentrations of Cd^{2+} in blood and urine showed significant differences among different groups (Figure 7C,D). In detail, trace Cd was determined in the blood and urine of mice from Group 1, probably due to the inherent Cd^{2+} in tap water or system errors during the detection. For Group 2, Cd^{2+} was accumulated in the fifth day and decreased by 56 and 40%, respectively, in the blood and urine in the ninth day due to the cessation of polluted water feeding. On the contrary, though Cd in mice of Group 4 were also enriched in the fifth day compared to that in Group 1, it was significantly lower than that in Group 2. With the help of living materials based on PM/6803, Cd in blood and urine of Group 4 was close to that in Group 1 (Figure 7C,D), which was not achieved in Group 3 using Ctr/6803. Furthermore, we investigated the behavioristics of mice, finding that the accumulation of Cd led to a slow-acting behavior in mice of Group 2, while it was significantly alleviated in Group 4 and partially alleviated in Group 3 (Figure 7E). Though *Synechocystis* sp. PCC 6803 has natural bioremediation ability for Cd, and we could see that the effect of using Ctr/6803 in Group 3 is poorer than that using PM/6803 in Group 4, suggesting that our engineered strain was also superior for in vivo use. Finally, we demonstrated the biosafety of PM/6803-based living materials via comparing the blood routine examination and pathological analysis of main organs including heart, liver, spleen, lung, and kidney in mice from Groups 1

https://doi.org/10.1021/acsnano.4c02493
ACS Nano 2024, 18, 17694−17706

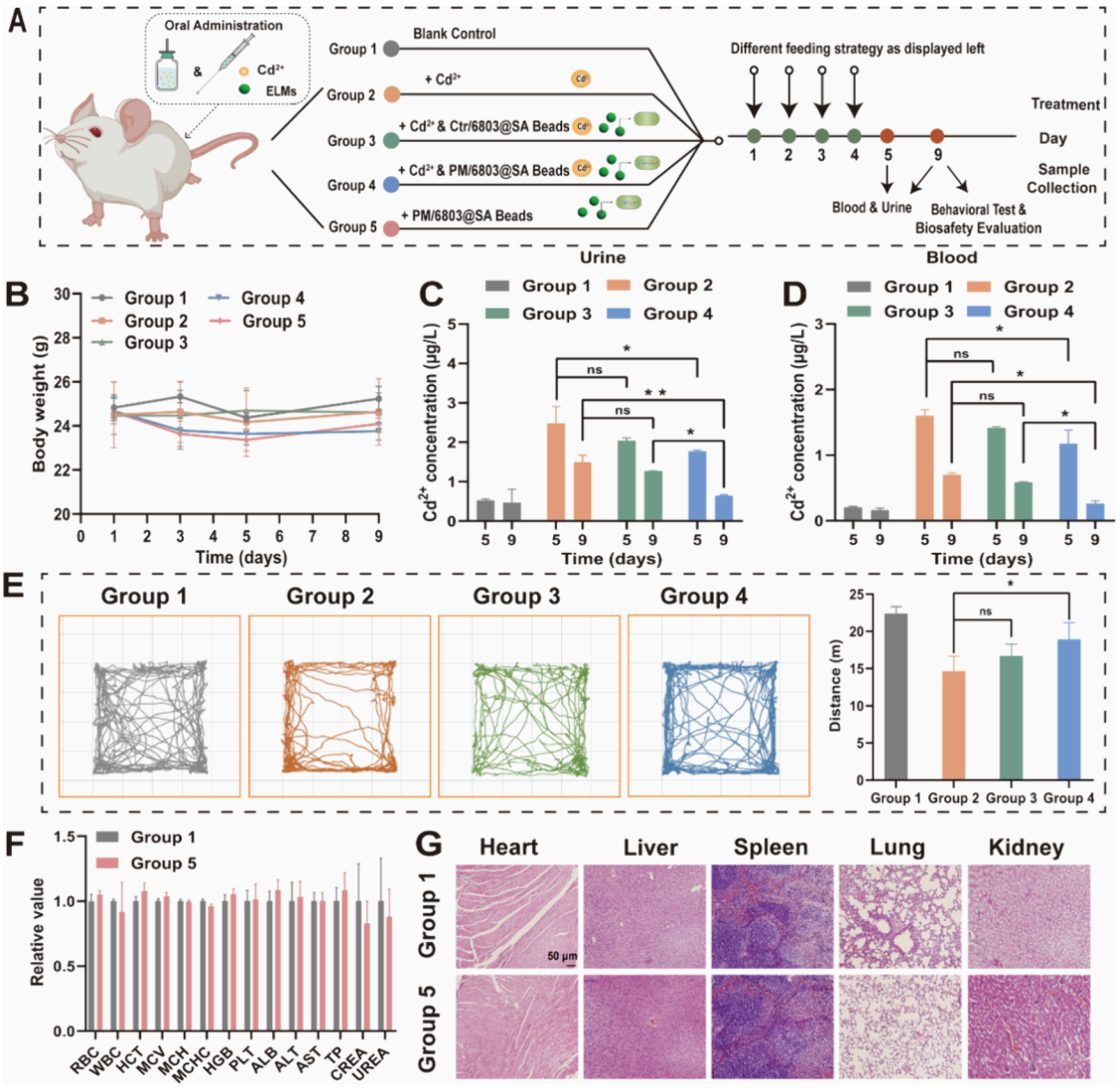

Figure 7. Application of PM/6803@SA for Cd^{2+} bioremediation using mice model. (A) Schematic of the evaluation of PM/6803 in Cd^{2+} bioremediation using mice mode. (B) Body weight of mice in different groups. Concentrations of Cd^{2+} in the blood (C) and urine (D) of mice in different groups at the fifth and ninth day. (E) Behavioral tests and the total distance count of mice in different groups at the ninth day. (F) Relative change of blood routine parameters in Group 1 and Group 4 at the ninth day. (G) Main organ comparisons between mice in Group 1 and Group 4 at the ninth day. (*$p < 0.05$ and **$p < 0.01$ by Student's t test).

and 4 (Figures 7F,G and S7). Our results indicated that PM/6803-based living materials were feasible and biocompatible for in vivo bioremediation of Cd^{2+}.

DISCUSSION

Rapid industrialization increases the possibilities of HMs pollution accidents in the world. In China, Cd pollution in Beijiang and Longjiang occurred in 2005 and 2012, respectively, causing great harm to aquatic organisms and threatening the water supply security and human health.[35] As a promising strategy, bioremediation of HMs via engineered microorganisms has attracted greater attention in recent years. Previously, surface display of a metal-specific binding protein like PbrR has been utilized for bioremediation of protein-cognate HMs like Pb^{2+}. For example, Wei et al. incorporated PbrR and promoter from the lead-resistant *pbr* operon of *Cupriavidus metallidurans* CH34 into *E. coli*,[8] allowing for absorbing Pb^{2+} up to 150 μM as well as a slight decreased binding capacity to Cd^{2+}. Furthermore, Sun et al. developed a strategy of bioremediation by controlling naturally occurring production of H_2S with yeast, which effectively absorbed Cu^{2+}, Zn^{2+}, Cd^{2+}, Pb^{2+}, and Hg^{2+} and bioremediated them intracellularly.[9] In this study, via utilizing the metal chelators PCS and MT, we also achieved bioremediation toward multiple HMs including Cd^{2+}, Cu^{2+}, and Zn^{2+}. Though PM/6803 did not target as many HMs as reported previously, its bioremediation capability for Cd^{2+} is the highest (about 279 μM) among the reported studies to our knowledge.

Heterotrophic *E. coli* and yeast depend on organic carbon sources not commonly survived in the polluted water for a long time.[35] In this case, photosynthetic cyanobacteria have a natural niche and could survive easier, which can allow for long-term treatment in a specific environment like sewage disposal plants or industrial wastewater. Meanwhile, cyanobacteria are easy to culture, whose cultivation cost is decreasing, approximately $281 per ton nowadays,[36] making it possible for generating PM/6803-based materials with a large scale. On the other hand, unexpected uptake of HMs in animals or humans

https://doi.org/10.1021/acsnano.4c02493
ACS Nano 2024, 18, 17694−17706

would occur due to drinking of the polluted water or enrichment via the food chain. Previously, Hui et al. engineered surface displayed PbrR in *E. coli*, realizing the in vivo bioremediation of Pb in mice models.[37] In this study, the bioremediation effects of PM-6803 were demonstrated via zebrafish models. We also demonstrated the feasibility of PM/6803-based living materials for in vivo bioremediation of Cd^{2+} via mice model. Previously, biosafety and biocompatibility of specific cyanobacterium like *Synechococcus elongatus* PCC 7942[38] and *Spirulina platensis*[24] have been demonstrated in various dependent studies. Here, we demonstrated the biosafety of the in vivo use of *Synechocystis* sp. PCC 6803; thus our engineered living materials may extend their application range in the future. Though it may still be far from clinical application on humans, it is possible to treat animals poisoned by HMs in the future.

Though some progress was made in this study, other approaches such as spatial expression of PCS and MT like surface display or their combination with other metal-binding proteins like PbrR are worth exploration in the future. Besides, some metal elements like Ag are lethal to bacteria including cyanobacteria due to its high antimicrobial activity.[39] In this case, artificial microcompartments can protect cells by isolating toxic products. Previously, Xing et al. constructed self-assembling nanocompartments in *E. coli*,[40] which achieved removal of Ag from water and a survival rate of engineered strain at 86% under 30 μM Ag^{+}. Moreover, Pi et al. recently proposed a strategy that converted the HMs in wastewater to create semiconductor biohybrids in situ for scalable solar-to-chemical production,[41] which could also be considered in cyanobacteria. Finally, to avoid the introduction of engineered strain during the treament, more effective hydrogels to exclude the escape of the engineered strain can be developed, which only allowed substances exchange.[42] Even though the hydrogel beads used in this study could be accidentally eaten by other organisms due to their small size. Therefore, biomaterials with a larger size can be designed and created in the future.

CONCLUSIONS

In this study, genes encoding two types of metal chelator proteins were introduced into the model cyanobacterium *Synechocystis* sp. PCC 6803, significantly enhancing its tolerance to heavy metals, including Cd^{2+}, Zn^{2+}, and Cu^{2+}. The bioremediation capacity of the engineered strain PM/6803 was demonstrated to be approximately 21 $\mu g/OD_{750}$ by using Cd^{2+} as a proof of concept. Furthermore, PM/6803 was stabilized as living material when encapsulated in sodium alginate-based hydrogels, showing promising results in bioremediating Cd^{2+} both in vitro using a zebrafish model and in vivo using a mice model. In the future, research could focus on developing engineered strains with more efficient bioremediation capacities and on creating biomaterials that allow the exchange of substances without the leakage of strains.

METHODS

Bacterial Growth Conditions. Normally, wild type *Synechocystis* sp. PCC 6803 and the engineered strains in this study were grown in BG11 medium (pH 7.5 or 9.0 as required) under a light intensity of 50 (μmol of photons/m^2)/s in an HNY-202t illuminating incubator of 130 rpm at 30 °C (Honor, Tianjin, China). *N*-[Tris-(hydroxymethyl)methyl]-2-aminoethanesulfonic acid (Solarbio, Beijing, China) was utilized to adjust the pH of the medium when needed. For growth patterns measurement, 5 mL of fresh cells at OD_{750} of 0.2 were collected by centrifugation and inoculated into 20 mL of BG11 liquid medium in a flask. A 200 μL aliquot of culture samples was taken every 24 h and measured at OD_{750} on an ELx808 Absorbance Microplate Reader (BioTek, VT, USA). Growth experiments were repeated at least 6 times to confirm the growth patterns. To maintain the stability of the constructed strains, 20 μg/mL spectinomycin was added when necessary. *E. coli* DH5α were grown on a standard LB agar plate in an incubator or in medium using an HNY-100B shaking incubator (Honor, Tianjin, China) with 100 μg/mL spectinomycin at 37 °C, respectively. For induction of the theophylline-responsive riboswitch, a stock solution of theophylline (Aladdin, Shanghai, China) was prepared at concentration of 10 mM dissolved in normal BG11 medium and diluted into a final concentration of 2 mM when used. For bioremediation investigation of Cd^{2+}, Cu^{2+}, or Zn^{2+}, a 1000X stock solution of $CdSO_4 \cdot (8/3)H_2O$ (Aladdin, Shanghai, China), $CuSO_4 \cdot 5H_2O$ (Kewei, Tianjin, China), or $ZnSO_4$ (Yuanye, Shanghai, China) was prepared and then added into the medium according to specific concentration(s), respectively.

Strains Construction. *E. coli* DH5α strain was used as a host for plasmid construction and amplification. A shuttle vector pJA2 with RSF1010 ori was used as a backbone.[43] *PCS* and *MT* respectively encoding phytochelatin (PCS) and metallothionein (MT) were both chemically synthesized, whose expressions were under the control of a theophylline-responsive promoter P_{tho}.[44] Three plasmids containing *PCS* or *MT* or their combination were constructed. For Western blotting, 6× His tag and 3× Flag tag were added to the N- and C-termini, respectively. Further, the constructed plasmids and a blank plasmid were introduced into *Synechocystis* sp. PCC 6803 by natural transformation (Table S1). The spectinomycin-resistant transformants were obtained and confirmed by colony PCR and sequencing analysis. Genetic cassettes used in this study were listed in Table S2.

SDS-PAGE. Cultures of PCS/6803, MT/6803, and PM/6803 after induction were respectively collected and broken by SCIENTZ-IID ultrasonic homogenizer (Scientz Biotechnology Co.,Ltd., Ningbo, China). The cell debris was removed by centrifugation at 10000*g* (4 °C, 10 min), and intracellular crude protein was obtained. The recombinant protein was purified with MagneHisTM Ni-particles (Promega, Beijing, China). The composition of elute buffer was 50 mM Tris, 300 mM NaCl, and 8 M urea adjusted to pH 8.0 with hydrochloric acid. The eluted proteins were collected and subjected to SDS-PAGE. A Coomassie Bright Blue Rapid dyeing solution (Shanghai Wansheng Haotian Biotechnology Co., Ltd., Shanghai, China) was used for protein glue color development.

Cell Dry Weight Measurement. Samples of Ctr/6803 and PM/6803 were collected after 6 days' cultivation under Cd^{2+} stress (0, 10, 15, or 25 μM Cd^{2+} was added at day 2). For measurement of cell dry weight, 20 mL samples were obtained by centrifugation (7000*g*; 10 min; 4 °C) and cell pellets were transferred to preweighed 1.5 mL centrifuge tubes followed by immediate liquid nitrogen freezing. The samples were dried using an LGJ-10 vacuum freeze drier (Songyuan Huaxing, Beijing, China) and reweighed.

Measurement of Chlorophyll *a* (Chl *a*), Carotenoids, Absorption Spectrum, and F_v/F_m. Samples of Ctr/6803 and PM/6803 were collected after 96 h of cultivation under Cd^{2+} stress (0, 10, 15, or 25 μM Cd^{2+} was added at day 2). To measure the Chl *a* and carotenoids content, cells (volume × OD_{750} = 0.5) were centrifuged at 15000*g* for 4 min at 4 °C to collect the pellets. A 1 mL aliquot of methanol (precooled at 4 °C) was used to resuspend the pellets, and the suspension was incubated at 4 °C for 20 min to extract the pigments. The supernatant was collected by centrifugation at 15000*g* and 4 °C for 10 min. Finally, the supernatant was measured at 470, 665, and 720 nm. The content of Chl *a* was calculated using the formula: Chl *a* [μg/mL] = dilution ratio × $12.9447(A_{665} - A_{720})$.[45] Carotenoids [$\mu g$/mL] = dilution ratio × $[1000(A_{470} - A_{720}) - 2.86(\text{content of Chl } a)]/221$.[46] To measure the absorption spectrum, cell densities were normalized with OD_{750} and measured on a UV-1601 spectrophotometer (Beifen-Ruili, Beijing, China). Data were analyzed by the UVprobe software (Version X). For F_v/F_m measurement, 1 mL samples were collected and transferred into the

https://doi.org/10.1021/acsnano.4c02493
ACS Nano 2024, 18, 17694−17706

AquaPen AP 110/C hand-held PAM fluorometer (FluorCam, Drásov, Czech Republic). The samples were treated in darkness for 10 min.

ROS and Singlet Oxygen Measurements. Samples of Ctr/6803 and PM/6803 were collected after 96 h cultivation under Cd^{2+} stress (0, 10, 15, or 25 μM Cd^{2+} was added at day 2). For ROS measurement, cell samples (volume × OD_{750} = 0.5) were harvested and measured using a Reactive Oxygen Species Assay Kit (Beyotime, Shanghai, China) following the manufacturer's protocol. Briefly, the 1 nonfluorescent probe DCFH-DA was finally oxidized by intracellular ROS or other peroxides fluorescent DCF. The DCF was detected using an F-2700 fluorescence spectrophotometer (Hitachi, Tokyo, Japan) at EX 488 nm and EM 525 nm. For singlet oxygen measurement, cell samples (volume × OD_{750} = 0.5) were harvested and measured using a SOSG singlet oxygen fluorescence probe (Meilun, Dalian, China) following the protocol. The SOSG stained sample was detected at EX 488 nm and EM 535 nm.

Microscope analysis and Identification of the Cd Nanomaterial. Transmission electron microscope (TEM) and scanning electron microscope (SEM) analysis were provided by Zhongke Baice Technology Co., Ltd. (Beijing, China). For sample preparation, Ctr/6803 and PM/6803 were collected by centrifugation (7500*g*; 10 min; 4 °C) after 2 days' cultivation with or without 10 μM Cd^{2+}. The cell pellets were transferred into a tube and washed twice using PBS buffer (pH 7.0; 0.1 M). Then, 1 mL of 2.5% (v/v) glutaraldehyde solution was added into the cell pellets and placed for 12 h at 4 °C. For TEM analysis, glutaraldehyde solution was removed and washed three times using PBS buffer. Briefly, the sample followed the process of fixation via osmic acid solution, cleaning using PBS buffer, dehydration through ethanol, and treatment of acetone and mixture of acetone and resin. The final sample was heated by gradient and cut into slices (70−90 nm) using UC7 Ultramicrotome (Leica, Wetzlar, Germany). The slices were stained with uranyl acetate solutions and lead citrate and then investigated on JE 1200-EX TEM (JEOL, Tokyo, Japan). For SEM analysis, glutaraldehyde solution was removed and washed three times using PBS buffer. Then the sample was dehydrated through ethanol and dried. Then the sample was investigated on SU8020 SEM (Hitachi, Tokyo, Japan). Automatic qualitative analysis was realized via EX-250 energy dispersive spectroscopy (HORIBA, Kyoto, Japan) combined with SEM.

Living Materials Preparation and Characterization. PM/6803 was collected after 7 days' cultivation (volume × OD_{750} = 0.5) and then resuspended with 15 mL of fresh BG11 medium. The resuspended sample was mixed with 30 mL of sodium alginate (2.5%, m/v) (the ratio of resuspended culture and sodium alginate was 1:2). Then the mixture was transferred into a sterile syringe to make microspheres via dropping them into 25% (m/v) $CaCl_2$ solutions. To make living materials with other shapes, a Z-603S FDM desktop 3D printer (JGAURORA, Shenzhen, China) was used to make a model made of 1.75 mm PLA plastic. The program for drawing the model was 3ds Max 2019. Then, the mixture of resuspended culture and sodium alginate was added to the model and solidified with 25% (m/v) $CaCl_2$ solutions. To track the viability of the cyanobacterium after being packaged, a small piece of the prepared living materials was cultured in BG 11 for continuous 5 days. The living materials were observed each day under the default ALEXA 633 channel of a confocal laser scanning microscope (Leica Stellaris 5, Germany) to obtain fluorescence images of the chlorophyll. The size of the PM/6803 beads was measured using a vernier caliper. The rheological analysis was provided by Zhongke Baice Technology Co., Ltd. (Beijing, China) using a rheometer (MCR92, Anton Paar, Austria). For characterization of the materials vis SEM, the prepared hydrogel materials were frozen at −80 °C for 24 h and then the sample was freeze-dried to remove residual moisture. The final sample was analyzed using SU8020 SEM (Hitachi, Tokyo, Japan). For microscopy analysis, the fluorescence images of 6803/PM@SA beads were obtained using confocal laser scanning microscopy (Leica Stellaris 5, Germany). The beads were stained with calcein (green), and PM/6803 was observed by chlorophyll autofluorescence (red).

Bioremediation Assays toward Cd^{2+}. Quantitation of the Cd^{2+} remaining in the medium/water or accumulating in the muscle of zebrafish was performed using an iCAP 7400 ICP-OES analyzer (ICP-OES; Thermo Fisher, Carlsbad, CA, USA). Briefly, standard Cd^{2+} solutions with gradient concentrations were prepared and measured and then used for sample quantitation (Figure S3).

For sample preparation with the medium (for culturing cyanobacteria) or water (for culturing zebra fish), 20 mL of supernatant of culture or water was collected via centrifugation and filtered using a 0.45 μm PES membrane and then for digestion with HNO_3 (Damao, Tianjin, China). Detailedly, the supernatant added with 3 mL of HNO_3 was treated under 170 °C for 2−3 h until the volume reached 2 mL due to the concentration. Then the digested solution was transferred to a 50 mL centrifuge tube and diluted into 20 mL with ddH_2O followed by detection via ICP-OES.

Wild-type zebrafish (TU; both male and female; six months old; 3.5 cm length on average) was purchased from GeneBio Co., Ltd. (Shanghai, China). The received zebrafish was precultured for 2 weeks using dechlorinated tap water (28.5 °C; pH 7.0−8.0; dissolved oxygen, 7.0 mg/L; light:dark = 14:10). Rich shrimp eggs were used as food. For Cd^{2+} exposure assays (5 mg/L), tap water was replaced with ddH_2O and feeding was stopped. For determining the Cd^{2+} in zebrafish, ones that died were stored at −20 °C and living ones were sacrificed at 24 h. All of the fish were washed twice using ddH_2O. Head and tail were removed from the body. The remaining body was weighted and digested with 3 mL ddH_2O, 5 mL of HNO_3, 3 mL of perchloric acid (Aladdin, Shanghai, China), and 3 mL of 30% H_2O_2 (Kermel, Tianjin, China) followed by detection via ICP-OES.

In the in vivo assays, female BALB/c mice (6−8 weeks old) were purchased from Gem Pharmatech Co., Ltd. (Nanjing, China). All animal experiments were operated following the Guidance Suggestions for the Care and Use of Laboratory Animals. The animal experiments were approved by the ethics committee of Xuzhou Medical University (Approval No. 202211S061). Mice were randomly divided into 5 groups. Mice in Group 2, Group 3, and Group 4 were orally administered Cd^{2+} water (5 mg/L). Mice in Group 3 were orally administered Ctr/6803 packaged hydrogels for 4 consecutive days. Mice in Group 4 were orally administered PM/6803 packaged hydrogels for 4 consecutive days. On the fifth and ninth days, blood and urine were collected for ICP-MS measurement (PerkinElmer NexION 300D, USA). To investigate the effects of Cd^{2+}, an open-field method was used for the behavioral tests. Briefly, on the ninth day, mice from Group 1, Group 2, Group 3, and Group 4 moved freely in an open place for 5 min, and the behavior was recorded and analyzed by ANY-maze software (Stoelting, USA). The in vivo biocompatibility of PM/6803 was evaluated by routine blood, biochemistry, and histopathology analysis. Mice in Group 5 were orally administrated PM/6803 packaged hydrogels for 4 consecutive days, and then blood samples were collected for blood routine and biochemistry analysis on the ninth day along with mice in Group 1. At the same time, mice in Group 1 and Group 5 were sacrificed and major organs were harvested for hematoxylin and eosin staining.

ASSOCIATED CONTENT

Supporting Information

The Supporting Information is available free of charge at https://pubs.acs.org/doi/10.1021/acsnano.4c02493.

(Figure S1) Verification of the constructed strains; (Figure S2) Growth patterns and energy dispersive spectroscopy analysis; (Figure S3) Cd^{2+} standard curve; (Figure S4) bioremediation abilities; (Figure S5) long-term stability evaluation; (Figure S6) ELM characterization; (Figure S7) mice blood routines and blood biochemical parameters; (Table S1) strains used; (Table S2) DNA sequence used (PDF)

https://doi.org/10.1021/acsnano.4c02493
ACS Nano 2024, 18, 17694−17706

AUTHOR INFORMATION

Corresponding Authors

Weiwen Zhang − *Laboratory of Synthetic Microbiology, School of Chemical Engineering & Technology and Center for Biosafety Research and Strategy, Tianjin University, Tianjin 300072, People's Republic of China; Frontier Science Center for Synthetic Biology & Key Laboratory of Systems Bioengineering, Ministry of Education of China, Tianjin 300072, People's Republic of China;* orcid.org/0000-0001-8305-5653; Phone: 0086-22-2740-6394; Email: wwzhang8@tju.edu.cn; Fax: 0086-22-2740-6364

Lei Chen − *Laboratory of Synthetic Microbiology, School of Chemical Engineering & Technology, Tianjin University, Tianjin 300072, People's Republic of China; Frontier Science Center for Synthetic Biology & Key Laboratory of Systems Bioengineering, Ministry of Education of China, Tianjin 300072, People's Republic of China;* orcid.org/0000-0003-1459-2329; Phone: 0086-22-2740-6364; Email: lchen@tju.edu.cn; Fax: 0086-22-2740-6394

Authors

Tao Sun − *Laboratory of Synthetic Microbiology, School of Chemical Engineering & Technology and Center for Biosafety Research and Strategy, Tianjin University, Tianjin 300072, People's Republic of China; Frontier Science Center for Synthetic Biology & Key Laboratory of Systems Bioengineering, Ministry of Education of China, Tianjin 300072, People's Republic of China;* orcid.org/0000-0002-7575-3483

Huaishu Huo − *Laboratory of Synthetic Microbiology, School of Chemical Engineering & Technology, Tianjin University, Tianjin 300072, People's Republic of China; Frontier Science Center for Synthetic Biology & Key Laboratory of Systems Bioengineering, Ministry of Education of China, Tianjin 300072, People's Republic of China*

Yingying Zhang − *School of Medical Imaging, Xuzhou Medical University, Xuzhou 221004 Jiangsu, People's Republic of China*

Yaru Xie − *Laboratory of Synthetic Microbiology, School of Chemical Engineering & Technology, Tianjin University, Tianjin 300072, People's Republic of China; Frontier Science Center for Synthetic Biology & Key Laboratory of Systems Bioengineering, Ministry of Education of China, Tianjin 300072, People's Republic of China*

Yize Li − *School of Medical Imaging, Xuzhou Medical University, Xuzhou 221004 Jiangsu, People's Republic of China*

Kungang Pan − *Laboratory of Synthetic Microbiology, School of Chemical Engineering & Technology, Tianjin University, Tianjin 300072, People's Republic of China; Frontier Science Center for Synthetic Biology & Key Laboratory of Systems Bioengineering, Ministry of Education of China, Tianjin 300072, People's Republic of China*

Fenfang Zhang − *Laboratory of Synthetic Microbiology, School of Chemical Engineering & Technology, Tianjin University, Tianjin 300072, People's Republic of China; Frontier Science Center for Synthetic Biology & Key Laboratory of Systems Bioengineering, Ministry of Education of China, Tianjin 300072, People's Republic of China*

Jing Liu − *School of Life Sciences, Tianjin University, Tianjin 300072, People's Republic of China*

Yindong Tong − *School of Environmental Science and Engineering, Tianjin University, Tianjin 300072, People's Republic of China;* orcid.org/0000-0002-0503-6585

Complete contact information is available at: https://pubs.acs.org/10.1021/acsnano.4c02493

Author Contributions

[▽]T.S., H.H., and Y.Z. contributed equally to this work.

Notes

The authors declare no competing financial interest.

ACKNOWLEDGMENTS

This research was supported by grants from the National Key Research and Development Program of China (Grant No. 2018YFA0903600) and the National Natural Science Foundation of China (Grant Nos. 32371486, 31972931, 3227091, and 32070083).

REFERENCES

(1) Qasem, N. A. A.; Mohammed, R. H.; Lawal, D. U. Removal of heavy metal ions from wastewater: a comprehensive and critical review. *npj Clean Water* **2021**, *4* (1), 36.

(2) Tchounwou, P. B.; Yedjou, C. G.; Patlolla, A. K.; Sutton, D. J. Heavy metal toxicity and the environment. *Exp. Suppl.* **2012**, *101*, 133−164.

(3) Genchi, G.; Sinicropi, M. S.; Lauria, G.; Carocci, A.; Catalano, A. The Effects of Cadmium Toxicity. *Int. J. Environ. Res. Public Health* **2020**, *17* (11), 3782.

(4) Kubier, A.; Wilkin, R. T.; Pichler, T. Cadmium in soils and groundwater: A review. *Appl. Geochem.* **2019**, *108*, 104388.

(5) Smolders, E.; Mertens, J. Cadmium. In *Heavy Metals in Soils*, 3rd ed.; Alloway, B. J., Ed.; Environmental Pollution, Vol. *22*; Springer: Dordrecht, The Netherlands, 2013; pp 283−311. DOI: 10.1007/978-94-007-4470-7_10.

(6) Natasha; Shahid, M.; Khalid, S.; Murtaza, B.; Anwar, H.; Shah, A. H.; Sardar, A.; Shabbir, Z.; Niazi, N. K. A critical analysis of wastewater use in agriculture and associated health risks in Pakistan. *Environ. Geochem. Health* **2023**, *45* (8), 5599−5618.

(7) Cui, J.; Xie, Y.; Sun, T.; Chen, L.; Zhang, W. Deciphering and engineering photosynthetic cyanobacteria for heavy metal bioremediation. *Sci. Total Environ.* **2021**, *761*, No. 144111.

(8) Wei, W.; Liu, X.; Sun, P.; Wang, X.; Zhu, H.; Hong, M.; Mao, Z. W.; Zhao, J. Simple whole-cell biodetection and bioremediation of heavy metals based on an engineered lead-specific operon. *Environ. Sci. Technol.* **2014**, *48* (6), 3363−3371.

(9) Sun, G. L.; Reynolds, E. E.; Belcher, A. M. Using yeast to sustainably remediate and extract heavy metals from waste waters. *Nat. Sustainability* **2020**, *3* (4), 303−311.

(10) Xue, Y.; Du, P.; Ibrahim Shendi, A. A.; Yu, B. Mercury bioremediation in aquatic environment by genetically modified bacteria with self-controlled biosecurity circuit. *J. Clean. Prod.* **2022**, *337*, No. 130524.

(11) Turnau, K.; Płachno, B. J.; Bień, P.; Świątek, P.; Dąbrowski, P.; Kalaji, H. Fungal symbionts impact cyanobacterial biofilm durability and photosynthetic efficiency. *Curr. Biol.* **2023**, *33*, 5257.

(12) Anjana, K.; Kaushik, A.; Kiran, B.; Nisha, R. Biosorption of Cr(VI) by immobilized biomass of two indigenous strains of cyanobacteria isolated from metal contaminated soil. *J. Hazard Mater.* **2007**, *148* (1−2), 383−386.

(13) Rezasoltani, S.; Champagne, P. An integrated approach for the phycoremediation of Pb(II) and the production of biofertilizer using nitrogen-fixing cyanobacteria. *J. Hazard. Mater.* **2023**, *445*, No. 130448.

(14) Checchetto, V.; Formentin, E.; Carraretto, L.; Segalla, A.; Giacometti, G. M.; Szabo, I.; Bergantino, E. Functional characterization and determination of the physiological role of a calcium-

dependent potassium channel from cyanobacteria. *Plant Physiol.* **2013**, *162* (2), 953−964.
(15) Tian, Q.; Wang, J.; Cui, L.; Zeng, W.; Qiu, G.; Hu, Q.; Peng, A.; Zhang, D.; Shen, L. Longitudinal physiological and transcriptomic analyses reveal the short term and long term response of *Synechocystis* sp. PCC6803 to cadmium stress. *Chemosphere* **2022**, *303* (Pt 1), No. 134727.
(16) Li, M.; Ma, C.; Yin, X.; Zhang, L.; Tian, X.; Chen, Q.; Wang, L. Investigating trivalent chromium biosorption-driven extracellular polymeric substances changes of *Synechocystis* sp. PCC 7806 by parallel factor analysis (PARAFAC) analysis. *Bioresour. Technol. Rep.* **2019**, *7*, No. 100249.
(17) Xu, C.; Sun, T.; Li, S.; Chen, L.; Zhang, W. Adaptive laboratory evolution of cadmium tolerance in Synechocystis sp. PCC 6803. *Biotechnol. Biofuels* **2018**, *11*, 205.
(18) Toth, T.; Zsiros, O.; Kis, M.; Garab, G.; Kovacs, L. Cadmium exerts its toxic effects on photosynthesis via a cascade mechanism in the cyanobacterium, *Synechocystis* PCC 6803. *Plant Cell Environ.* **2012**, *35* (12), 2075−2086.
(19) Cobbett, C.; Goldsbrough, P. Phytochelatins and metallothioneins: roles in heavy metal detoxification and homeostasis. *Annu. Rev. Plant Biol.* **2002**, *53*, 159−182.
(20) Choi, Y.; Park, T. J.; Lee, D. C.; Lee, S. Y. Recombinant *Escherichia coli* as a biofactory for various single- and multi-element nanomaterials. *Proc. Natl. Acad. Sci. U. S. A.* **2018**, *115* (23), 5944−5949.
(21) Sun, T.; Zhang, Y.; Zhang, C.; Wang, H.; Pan, H.; Liu, J.; Li, Z.; Chen, L.; Chang, J.; Zhang, W. Cyanobacteria-Based Bio-Oxygen Pump Promoting Hypoxia-Resistant Photodynamic Therapy. *Front. Bioeng. Biotechnol.* **2020**, *8*, 237.
(22) Cohen, J. E.; Goldstone, A. B.; Paulsen, M. J.; Shudo, Y.; Steele, A. N.; Edwards, B. B.; Patel, J. B.; MacArthur, J. W., Jr.; Hopkins, M. S.; Burnett, C. E.; et al. An innovative biologic system for photon-powered myocardium in the ischemic heart. *Sci. Adv.* **2017**, *3* (6), No. e1603078.
(23) Zhong, D.; Zhang, D.; Chen, W.; He, J.; Ren, C.; Zhang, X.; Kong, N.; Tao, W.; Zhou, M. Orally deliverable strategy based on microalgal biomass for intestinal disease treatment. *Sci. Adv.* **2021**, *7* (48), No. eabi9265.
(24) Zhang, D.; Zhong, D.; Ouyang, J.; He, J.; Qi, Y.; Chen, W.; Zhang, X.; Tao, W.; Zhou, M. Microalgae-based oral microcarriers for gut microbiota homeostasis and intestinal protection in cancer radiotherapy. *Nat. Commun.* **2022**, *13* (1), 1413.
(25) Hirata, K.; Tsuji, N.; Miyamoto, K. Biosynthetic regulation of phytochelatins, heavy metal-binding peptides. *J. Biosci. Bioeng.* **2005**, *100* (6), 593−599.
(26) Habjanič, J.; Mathew, A.; Eberl, L.; Freisinger, E. Deciphering the Enigmatic Function of Pseudomonas Metallothioneins. *Front. Microbiol.* **2020**, *11*, 1709.
(27) Motta-Romero, H. A.; Perez-Donado, C. E.; Auchtung, J. M.; Rose, D. J. Toxicity of cadmium on dynamic human gut microbiome cultures and the protective effect of cadmium-tolerant bacteria autochthonous to the gut. *Chemosphere* **2023**, *338*, No. 139581.
(28) Tao, Y.; He, M.; Chen, B.; Ruan, G.; Xu, P.; Xia, Y.; Song, G.; Bi, Y.; Hu, B. Evaluation of Cd(2+) stress on *Synechocystis* sp. PCC6803 based on single-cell elemental accumulation and algal toxicological response. *Aquat. Toxicol.* **2023**, *258*, No. 106499.
(29) Schützendübel, A.; Polle, A. Plant responses to abiotic stresses: heavy metal-induced oxidative stress and protection by mycorrhization. *J. Exp. Bot.* **2002**, *53* (372), 1351−1365.
(30) Du, J.; Qiu, B.; Pedrosa Gomes, M.; Juneau, P.; Dai, G. Influence of light intensity on cadmium uptake and toxicity in the cyanobacteria *Synechocystis* sp. PCC6803. *Aquat. Toxicol.* **2019**, *211*, 163−172.
(31) Li, L.; Yang, C.; Ma, B.; Lu, S.; Liu, J.; Pan, Y.; Wang, X.; Zhang, Y.; Wang, H.; Sun, T.; et al. Hydrogel-Encapsulated Engineered Microbial Consortium as a Photoautotrophic "Living Material" for Promoting Skin Wound Healing. *ACS Appl. Mater. Interfaces* **2023**, *15* (5), 6536−6547.
(32) Gao, X.; Guo, C.; Hao, J.; Zhao, Z.; Long, H.; Li, M. Adsorption of heavy metal ions by sodium alginate based adsorbent-a review and new perspectives. *Int. J. Biol. Macromol.* **2020**, *164*, 4423−4434.
(33) Yin, H.; Chen, C. Y.; Liu, Y. W.; Tan, Y. J.; Deng, Z. L.; Yang, F.; Huang, F. Y.; Wen, C.; Rao, S. S.; Luo, M. J.; et al. *Synechococcus elongatus* PCC7942 secretes extracellular vesicles to accelerate cutaneous wound healing by promoting angiogenesis. *Theranostics* **2019**, *9* (9), 2678−2693.
(34) Özugur, S.; Chávez, M. N.; Sanchez-Gonzalez, R.; Kunz, L.; Nickelsen, J.; Straka, H. Green oxygen power plants in the brain rescue neuronal activity. *iScience* **2021**, *24* (10), 103158.
(35) Zhao, X. M.; Yao, L. A.; Ma, Q. L.; Zhou, G. J.; Wang, L.; Fang, Q. L.; Xu, Z. C. Distribution and ecological risk assessment of cadmium in water and sediment in Longjiang River, China: Implication on water quality management after pollution accident. *Chemosphere* **2018**, *194*, 107−116.
(36) Long, B.; Fischer, B.; Zeng, Y.; Amerigian, Z.; Li, Q.; Bryant, H.; Li, M.; Dai, S. Y.; Yuan, J. S. Machine learning-informed and synthetic biology-enabled semi-continuous algal cultivation to unleash renewable fuel productivity. *Nat. Commun.* **2022**, *13* (1), 541.
(37) Hui, C.; Guo, Y.; Zhang, W.; Gao, C.; Yang, X.; Chen, Y.; Li, L.; Huang, X. Surface display of PbrR on *Escherichia coli* and evaluation of the bioavailability of lead associated with engineered cells in mice. *Sci. Rep* **2018**, *8* (1), 5685.
(38) Liu, Y.; Zhong, D.; He, Y.; Jiang, J.; Xie, W.; Tang, Z.; Qiu, J.; Luo, J.; Wang, X. Photoresponsive Hydrogel-Coated Upconversion Cyanobacteria Nanocapsules for Myocardial Infarction Prevention and Treatment. *Adv. Sci. (Weinh)* **2022**, *9*, No. e2202920.
(39) Deng, H.; McShan, D.; Zhang, Y.; Sinha, S. S.; Arslan, Z.; Ray, P. C.; Yu, H. Mechanistic Study of the Synergistic Antibacterial Activity of Combined Silver Nanoparticles and Common Antibiotics. *Environ. Sci. Technol.* **2016**, *50* (16), 8840−8848.
(40) Xing, C. Y.; Ma, T. F.; Guo, J. S.; Shen, Y.; Yan, P.; Fang, F.; Chen, Y. P. Bacterially self-assembled encapsulin nanocompartment for removing silver from water. *Water Res.* **2021**, *191*, No. 116800.
(41) Pi, S. S.; Yang, W. J.; Feng, W.; Yang, R. J.; Chao, W. X.; Cheng, W. B.; Cui, L.; Li, Z. D.; Lin, Y. L.; Ren, N. Q. Solar-driven waste-to-chemical conversion by wastewater-derived semiconductor biohybrids. *Nat. Sustainability* **2023**, *6*, 1673.
(42) Tang, T.-C.; Tham, E.; Liu, X.; Yehl, K.; Rovner, A. J.; Yuk, H.; de la Fuente-Nunez, C.; Isaacs, F. J.; Zhao, X.; Lu, T. K. Hydrogel-based biocontainment of bacteria for continuous sensing and computation. *Nat. Chem. Biol.* **2021**, *17*, 724.
(43) Anfelt, J.; Hallstrom, B.; Nielsen, J.; Uhlen, M.; Hudson, E. P. Using transcriptomics to improve butanol tolerance of *Synechocystis* sp. strain PCC 6803. *Appl. Environ. Microbiol.* **2013**, *79* (23), 7419−7427.
(44) Sun, T.; Li, S.; Song, X.; Pei, G.; Diao, J.; Cui, J.; Shi, M.; Chen, L.; Zhang, W. Re-direction of carbon flux to key precursor malonyl-CoA via artificial small RNAs in photosynthetic *Synechocystis* sp. PCC 6803. *Biotechnol. Biofuels* **2018**, *11* (1), 26.
(45) Ritchie, R. J. Consistent sets of spectrophotometric chlorophyll equations for acetone, methanol and ethanol solvents. *Photosynth. Res.* **2006**, *89* (1), 27−41.
(46) Wellburn, A. R. The Spectral Determination of Chlorophylls a and b, as well as Total Carotenoids, Using Various Solvents with Spectrophotometers of Different Resolution. *J. Plant Physiol.* **1994**, *144* (3), 307−313.

https://doi.org/10.1021/acsnano.4c02493
ACS Nano 2024, 18, 17694−17706